Two-dimensional island wake experiments using distinct bathymetric domains representative of the island of Gran Canaria, Spain

UNIVERSIDAD DE LAS PALMAS DE GRAN CANARIA
Departamento de Física

E. Mason[1], P. Sangrà[1], Á. Peliz[2] and C. Dong[3]

[1] Departamento de Física, Universidad de Las Palmas de Gran Canaria, Las Palmas, Spain

[2] Departamento de Física, Universidade de Aveiro, Aveiro, Portugal

[3] Institute of Geophysics and Planetary Physics, UCLA, California, U.S.A

Email: evan.mason101@doctorandos.ulpgc.es

1. Introduction

ROMS is being used within the project Remolinos Oceánicos Deposición Atmosférico (RODA) at the University of Las Palmas de Gran Canaria to gain a better understanding of the dynamics of eddy generation, shedding and subsequent evolution, at the island of Gran Canaria (GC). The RODA study region is the Canary Basin, where the Canary Island archipelago constitutes a natural barrier to the southwestward-flowing Canary Current (CaC); interaction between the islands and the CaC provokes an intense and complex eddy field in the southern downstream area (**Fig. 1**). We are in an early stage of this work and, in this poster, present results from a series of 2-D semi-idealised simulations. See the Website http://www.utm.csic.es/ for more about RODA.

2. Theoretical background

Gran Canaria's roughly circular shape is convenient as much of the theory for rotating flow past obstacles is for circular cylinders. The non-dimensional Reynolds number (Re) determines the form of a horizontal, uniform-density flow passing over an obstacle in a non-rotating frame (Batchelor, 1967):

$$\mathbf{Re = UD/A_H},$$

where U is upstream velocity, D the diameter of the obstacle, and A_H the horizontal eddy viscosity. Rotation is important in our experiments, and so we also consider the Rossby (Ro) and Ekman (Ek) numbers. Ro compares inertial to Coriolis forces:

$$\mathbf{Ro = U/fD},$$

where *f* is the Coriolis parameter. Ek compares viscous forces to the Coriolis forces:

$$\mathbf{Ek = A_H/D^2 f}.$$

Heywood *et al*. (1996) showed in an island wake modelling study that for Re < ~40 no eddies are generated; for ~40 < Re < ~100 eddies are generated when Ek and Ro tend away from zero and; for Re > ~100, eddies are generated unless either (Ek, Ro)→0. Note that Re = Ro/Ek, thereby determining the ratio of inertial to viscous forces.

Finally, the Strouhal number, **St=U/*n*D**, where *n* is the eddy shedding frequency (e.g., Tritton, 1988), provides a non-dimensional measure of the frequency of eddy shedding. The GC island wake problem is a deep-water wake problem, where the contribution of bottom drag to vorticity generation is considered to be inferior to that of lateral friction by the island flanks (e.g., Tomczak, 1988).

3. Modelling setup and experiments

Two sets of 26 experiments were carried out (**Tab. 1**). The first set is the flat bottom case (FBC) experiments where the domain comprises a flat bottom everywhere, with a land mask representing GC (**Fig. 2**). The second set is the partial bathymetry case (PBC) where real bathymetry is employed in the immediate region surrounding GC (**Fig. 2**) while the rest of the domain is again flat. The two domains are otherwise identical, with depth 2000 m (this is the approximate depth of the passages separating Gran Canaria from the adjacent islands of Tenerife and Fuerteventura; the CaC flows in the upper ~800 m), and horizontal dimensions of 710 x 450 km² (**Fig. 6** shows the full domain). The grid has 190 x 120 grid points, giving a mean grid resolution of ~3.7 km. The GC land mask is 14 grid cells wide in the N-S direction; the island, which lies 32 grid points from the western inflow boundary, has diameter ~50 km. Note that, for convenience, we rotate the entire domain ~120° anticlock wise.

Table 1. Model parameters. The incident speed, eddy viscosity, equivalent latitude of Coriolis parameter and non-dimensional parameters for the flat bottom (FBC) and partial bathymetry (PBC) flows past Gran Canaria. For PBC6 eddy shedding was irregular, hence no Strouhal number presented.

Run #	U_0 ($m\ s^{-1}$)	A_H ($m^2\ s^{-1}$)	Latitude (deg. N)	Re. #	Ro. #	Ek. (horiz.)	FBC St. #	FBC Mean lift coef.	FBC Mean drag coef.	PBC St. #	PBC Mean lift coef.	PBC Mean drag coef.
1	0,05	25	28	100	0,015	0,0003	0,174	0,92	1,76	n/a	0,72	-1,27
2	0,10	25	28	200	0,029	0,0003	0,179	0,53	1,55	n/a	0,07	-0,39
3	0,15	25	28	300	0,044	0,0003	0,188	0,45	1,63	n/a	0,07	0,06
4	0,20	25	28	400	0,059	0,0003	0,192	0,39	1,66	n/a	0,28	0,36
5	0,25	25	28	500	0,073	0,0003	0,197	0,35	1,70	n/a	0,17	0,49
6	0,30	25	28	600	0,088	0,0003	0,198	0,31	1,72	n/a	0,32	0,57
7	0,05	50	28	50	0,015	0,0006	0,154	0,78	1,84	n/a	0,96	-3,09
8	0,10	50	28	100	0,029	0,0006	0,161	0,37	1,51	n/a	-0,02	-1,16
9	0,15	50	28	150	0,044	0,0006	0,175	0,27	1,48	n/a	-0,14	-0,25
10	0,20	50	28	200	0,059	0,0006	0,178	0,23	1,52	n/a	0,14	0,27
11	0,25	50	28	250	0,073	0,0006	0,187	0,21	1,59	n/a	0,30	0,50
12	0,30	50	28	300	0,088	0,0006	0,191	0,20	1,63	0,128	0,35	0,59
13	0,05	100	28	25	0,015	0,0012	n/a	0,64	2,04	n/a	0,41	-4,96
14	0,10	100	28	50	0,029	0,0012	0,151	0,29	1,59	n/a	-0,60	-2,16
15	0,15	100	28	75	0,044	0,0012	0,154	0,18	1,44	n/a	-0,73	-0,76
16	0,20	100	28	100	0,059	0,0012	0,166	0,13	1,42	n/a	-0,36	0,04
17	0,25	100	28	125	0,073	0,0012	0,168	0,11	1,42	n/a	0,11	0,43
18	0,30	100	28	150	0,088	0,0012	0,175	0,10	1,45	n/a	0,35	0,59
19	0,25	50	10	250	0,198	0,0016	0,186	0,04	1,58	0,145	0,10	1,86
20	0,25	50	20	250	0,101	0,0008	0,186	0,14	1,59	0,133	0,44	0,72
21	0,25	50	30	250	0,069	0,0006	0,187	0,23	1,59	n/a	0,31	0,46
22	0,25	50	40	250	0,053	0,0004	0,187	0,32	1,59	n/a	0,21	0,25
23	0,25	50	50	250	0,045	0,0004	0,187	0,39	1,60	n/a	0,09	0,10
24	0,25	50	60	250	0,040	0,0003	0,187	0,45	1,60	n/a	0,04	0,02
25	0,25	50	70	250	0,037	0,0003	0,187	0,49	1,60	n/a	0,01	-0,02
26	0,25	50	80	250	0,035	0,0003	0,187	0,52	1,61	n/a	0,00	-0,04

A sea surface slope is imposed at the western (inflow) boundary, inducing an eastward incident current that flows toward and around the island. A no-slip condition is used at the island boundary. For the domain external boundary the Flather condition is used, with a sponge layer at the eastern (outflow) boundary. The Coriolis parameter is constant across the domain, set equivalent to 28°N unless otherwise indicated.

Details of the parameters used for individual runs are shown in **Tab. 1**. For both FBC and PBC, we conducted 3 series of 6 experiments where, for each series, the horizontal eddy viscosity was varied (A_H = 25, 50, 100 m² s⁻¹). Within each series, the incident flow was varied (U_0 = 0.05, 0.1, 0.15, 0.2, 0.25, 0.3 m s⁻¹). A final series of 8 experiments used Coriolis parameters corresponding to latitudes of 10, 20, 30, 40, 50, 60, 70 and 80°N, with A_H = 50 m² s⁻¹ and U_0 = 0.25 m s⁻¹. Each experiment lasts 74 model days, with dt = 16 s. Base case experiments are FBC11 and PBC11: here Re = 250, A_H = 50 m² s⁻¹, U_0 = 0.25 m s⁻¹, latitude = 28°N. Results from these runs are shown in Figures 3-8.

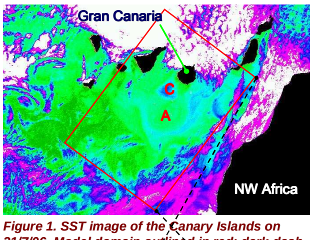

Figure 1. SST image of the Canary Islands on 31/7/06. Model domain outlined in red; dark-dash arrows to Fig. 2 indicate domain rotation. Note intense mesoscale acitivity to south of islands; cyclonic (C) and anticyclonic (A) eddies indicated to south of Gran Canaria.

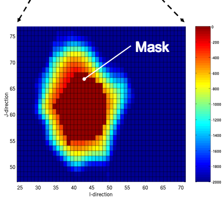

Figure 2. Zoom of Gran Canaria land mask, showing bathymetry used for partial bathymetry experiments.

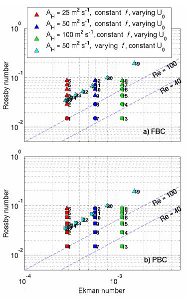

Figure 3. Ro/Ek flow regime diagrams showing Re of 40 and 100. Results are shown for (a) flat bottom and (b) partial bathymetry experiments. Triangles denote eddy shedding, circles denote wake fluctuations (for FBC decaying at smaller Re) and squares denote no eddy shedding.

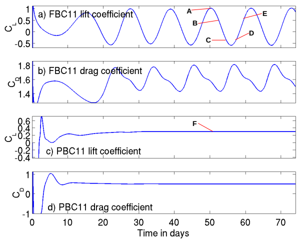

Figure 4. Time series of lift and drag coefficients for flat bottom (a, b) and partial bathymetry (c, d) simulations at Re = 250. (a, c) show the timestamps for the vorticity plots in Fig. 6.

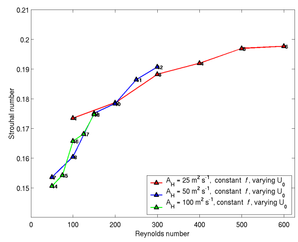

Figure 5. Strouhal number against Reynolds number for the flat bottom experiments.

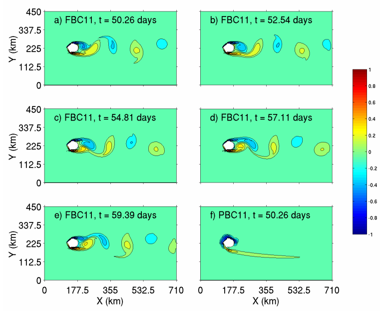

Figure 6. Vorticity fields, normalised by f, at the timestamps marked in Fig. 4 for the flat bottom [(a) through (e)] and partial bathymetry (f) simulations at Re = 250.

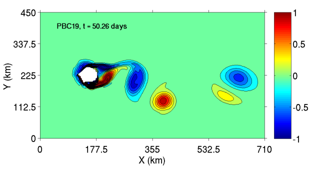

Figure 7. Vorticity field, normalised by f, for partial bathymetry run #19, where eddy shedding occurred. Compare with Fig. 6f.

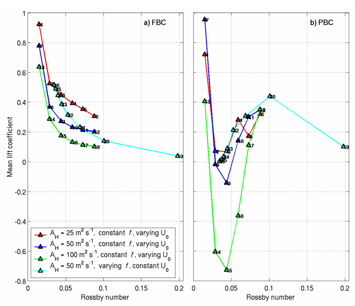

Figure 8. Mean lift coefficients against Rossby number for the flat bottom (a) and partial bathymetry (b) simulations.

4. Results

Fig. 3 shows regime diagrams of the FBC and PBC runs in dimensionless parameter space (Ek and Ro). For the FBC, **Fig. 3a** indicates FBC13 (lowest Re) having a non-fluctuating pair of attached eddies in the lee of the island; with increases of Re (FBC7, 14) the wake becomes unsteady, fluctuating periodically; the frequency of the fluctuations increases until, at Re = ~100 separation occurs, and eddies are shed from the island. **Fig. 3a** is qualitatively similar to Fig. 10 of Heywood *et al*. (1996). **Fig. 3b** indicates that PBC eddy shedding only occurred in 4 experiments, namely PBC6, 12, 19 and 20. Taylor-Proudman theory (e.g., Baines and Davis, 1980) states that as (Ek, Ro)→0, Taylor columns are formed in a homogeneous fluid flowing over an obstacle. In the majority of the PBC experiments, the formation of Taylor-column like flow around the island (see **Fig. 6f**) appears to suppress the eddy generation mechanism.

Lift and drag forces created when the current passes around the island may be described by the respective coefficients, C_L and C_D. We follow Dong *et al*. (2006) in calculating these coefficients for each experiment (**Tab. 1**). Time evolutions for C_L and C_D for FBC11, where Re = 250, are shown in **Fig. 4a, b**. After an initialisation period of just over 20 days, both C_L and C_D oscillate at a constant rate around a stationary mean value, owing to the contributions of the upper and lower alternating vortices to the drag. The mean CL oscillations are equivalent to the St frequency which equals 0.186; Heywood *et al*. (1996) obtained St = 0.179 for a circular island at Re = 252. All St are plotted against Re in **Fig. 5**; the shedding frequency increases with Re. For a circular land mask, the frequency of the C_D oscillations is double that of C_L (not shown); in our case, this effect is noticeable as a slight 'bump' repeatedly seen in the C_D curve of **Fig. 4b**. The amplitudes of the mean C_L and C_D curves increase as Re increases. In contrast to FBC11, the PBC11 C_L and C_D time series in **Fig. 4c, d** are flat, indicating no eddy shedding/wake fluctuation.

Fig. 6a-e shows a sequence of vorticity fields corresponding to the time steps indicated on **Fig. 4a**. The subfigures show the evolution of the vorticity field over a shedding period (~11.4 days); an anticyclonic eddy is generated and released from the north, followed by a cyclonic eddy from the south. Wake asymmetry is evident, the cyclonic eddies are more intense than the anticyclonic (e.g., Chabert D'Hieres *et al*., 1989). **Fig. 6f** shows the temporally-corresponding PBC11 vorticity field, which is stationary in time, unlike the FBC. Such wakes have been seen in numerical studies of flow around seamounts (e.g., Goldner & Chapman, 1997). For comparison, **Fig. 7** shows the vorticity field for an eddy-shedding PBC run, PBC19; here the Coriolis parameter is small, so that Taylor column generation is minimised, permitting eddies to develop.

Mean values of C_L for FBC and PBC are plotted against Ro in **Fig. 8a, b**. For all FBC, C_L remains positive (acting northward) but decreases with decreasing rotation. This is particularly evident in the varying *f* runs, where C_L rapidly increases as *f* increases. A high mean C_L indicates increased asymmetry between cyclonic and anticyclonic vortices, cyclonics being more intense. C_L is also seen to be influenced by changes in A_H: C_L is stronger for smaller A_H, and vice-versa.

For PBC (**Fig. 8b**), the constant *f* runs show C_L initially decreasing sharply, before increasing again for Ro >= 0.04. Different values for A_H do not separate out the curves as clearly as they do for FBC, particularly for A_H = 25 and 50 m² s⁻¹. Both the A_H = 50- and 100-m²-s⁻¹ runs achieve negative values (acting southward); at A_H = 100 m² s⁻¹, C_L is less than -0.7 for Ro = 0.044. C_L increases as *f* decreases until latitude 20°N, whereafter it decreases again.

5. Conclusions

- Using ROMS in 2-D mode, we are able to generate an eddy field in the downstream wake of an obstacle representative of the island of Gran Canaria.
- Profound differences observed in the circulation between the flat bottom (FBC) and partial bathymetry (PBC) experiments; Taylor-column-like circulation dominates for the PBC runs, strongly inhibiting eddy shedding.
- For both cases, increasing viscosity and rotation tends to reduce eddy formation, although the ranges are markedly different.
- Strouhal numbers are in agreement with theoretical predictions and numerical studies (e.g., Williamson, 1996; Heywood *et al*., 1996).
- Recent estimates put the mean velocity of the CaC at 0.05 m s⁻¹ and A_H at 25 m² s⁻¹ (Sangrà *et al*., 2005). These give Re = 100, equivalent to FBC1/PBC1; eddy shedding does not occur in either of these runs (see **Fig. 3**). In other words, the model in its present form does not produce the observed eddy field (e.g., **Fig. 1**). This is a long-standing problem for GC (e.g., Sangrà, 1995) which we plan to address using 3-D ROMS simulations that will include wind forcing, an important secondary source of vorticity generation.

6. Acknowledgements

Evan Mason is supported by a Spanish Ministry of Education and Science FPI grant. 2-minute Gridded Global Relief Data (ETOPO2v2) data provided by the U.S. Department of Commerce, National Oceanic and Atmospheric Administration, National Geophysical Data Center, 2006.; from their website at http://www.ngdc.noaa.gov/.

7. References

1. Baines P.G.; Davies P.A. (1980): Laboratory studies of topographic effects in rotating and/or stratified fluids. In "*Orographic effects in planetary flows*", ed. Hide R.; White P., WMO, 23, GARP Publ. Ser., Geneva, 233-299.
2. Batchelor G.K. (1967): An introduction to fluid mechanics, 1st Ed., Cambridge University Press, Cambridge, U.K.; 615 pp.
3. Chabert D'Hieres G.; Davies P.A.; Didele H. (1989): A laboratory study of the lift forces on a moving solid obstacle in a rotating fluid. *Dynamics of Atmospheres and Oceans*, **13**, 47–75.
4. Dong C.; McWilliams J.C.; Shchepetkin A.F. (2006): Island wakes in deep water, submitted to *Journal of Physical Oceanography*.
5. Goldner D.R.; Chapman D.C. (1997): Flow and particle motion induced above a tall seamount by steady and tidal background currents. *Deep Sea Research I*, **44**(5), 719–744.
6. Heywood K.J.; Stevens D.P.; Bigg G.R. (1996): Eddy formation behind the tropical island of Aldabra. *Deep-Sea Research Part I*, **43**(4), 555-578.
7. Sangrà P. (1995): Perturbación de un flujo geofísico por un obstáculo: Aplicación a la isla de Gran Canaria. Universidad de Las Palmas de Gran Canaria, *Tesis doctoral*, 201pp.
8. Sangrà P.; Pelegrí J.L.; Hernández-Guerra A.; Arregui I.; Martín J.M.; Marrero-Díaz A.; Martínez A.; Ratsimandresy A.W.; Rodríguez-Santana A. (2005): Life history of an anti-cyclonic eddy. *Journal of Geophysical Research*, **110**, C03021.
9. Tomczak M. (1988): Island wakes in deep and shallow water. *Journal of Geophysical Research*, **93**(C5), 5153-5154.
10. Tritton D.J. (1988): Physical fluid dynamics. 2nd Ed., Oxford Science Publications, 519pp.
11. Williamson C.H.K. (1996): Vortex dynamics in the cylinder wake. *Annual Review of Fluid Mechanics*, **28**, 477-539.